Available online at www.easdprocedia.org
EASD Procedia EURODYN (2020) 1791-1804

EASD Procedia

EURODYN 2020
XI International Conference on Structural Dynamics
M. Papadrakakis, M. Fragiadakis, C. Papadimitriou (eds.)
Athens, Greece, 23–26 November 2020

MEASURING THE DYNAMIC RESPONSE OF A LIVELY FOOTBRIDGE TO AMBIENT AND WALKING EXCITATION

Alfredo Cigada[1], Carmelo Gentile[2], Giulia Lastrico[3] and Maria Gabriella Mulas[3]

[1] Dept. of Mechanical Engineering (DMEC), Politecnico di Milano
Via La Masa 1 Milano, Italy
e-mail: alfredo.cigada@polimi.it

[2] Dept. of Architecture, Built Environment and Construction Engng. (DABC), Politecnico di Milano,
Piazza Leonardo da Vinci 32, 20133 Milano, Italy
e-mail: carmelo.gentile@polimi.it

[3] Department of Civil and Environmental Engineering (DICA), Politecnico di Milano
Piazza Leonardo da Vinci 32, 20133 Milano, Italy
e-mail: giulia.lastrico@polimi.it; mariagabriella.mulas@polimi.it

Keywords: Lively footbridge; ambient vibration tests, forced vibration tests; walking pedestrians; resonant conditions.

Abstract. *The paper presents selected results of a first experimental campaign on a footbridge over-passing the Lambro River near Milano (Italy). The 3-span footbridge, for a bicycle-pedestrian mixed use, has a reinforced concrete deck supported by a steel structure. The footbridge, 107 m long and with a constant width of 4.4m, is roughly symmetric about both mid-span and the longitudinal axis. As a part of proof tests performed in March 2016, ambient vibration tests identified the footbridge modal properties, detecting at 1.75 Hz the fundamental bending mode with the maximum amplitude recorded at mid-span, a finding confirmed by an ANSYS FE model of the footbridge. A series of forced vibration tests, performed in July 2017, investigated the response of the bridge under different loading conditions. Groups of pedestrians, in number of 1, 2, 3, 4, 6, 8 and 12, crossed the bridge, walking with a step frequency as close as possible to the first fundamental frequency. Different spatial configurations were explored for each number of pedestrians, investigating the spread in data related to different walking people/groups and their formation. Pedestrians followed straight trajectories and their spatial configuration was symmetric about the longitudinal axis of the bridge; single pedestrians walked along the footbridge axis. This paper focuses on a few results related to: (a) single pedestrians; (b) groups of multiple pedestrians in the same configuration, a longitudinal row; (c) 12 pedestrians in different spatial configurations. Experimental results highlight the effect of both intra-subject and inter-subject variability and the influence of spatial configuration on the maximum measured acceleration. The bridge performance is discussed by comparison between experimental results and limit values of the vertical acceleration according to HiVoSS guideline.*

ISSN:2311-9020
Peer-review under responsibility of the Organizing Committee of EURODYN 2020.
doi: 10.47964/1120.9144.19087

INTRODUCTION

In the last two decades, dynamic testing of bridges has been widely adopted for several purposes, as in identification of dynamic properties in proof tests, validation of FE models, and detection of excessive vibrations for lively footbridges [1]-[5]. Very often, aesthetic aspects have motivated the structural conception of recent footbridges, characterized by significant slenderness. For this reason, a significant amount of research work has been devoted to the problem of their serviceability assessment [6], also because slender structures are prone to a modification of modal properties due to the increase of mass when pedestrians are present [7]. In addition, the problem of human-structure interaction requires the derivation of proper pedestrian models and procedures of analysis [8], [9].

This paper presents selected results of a research work that covers many of the above aspects with reference to a footbridge located in Northern Italy. Ambient vibration tests (AVTs) performed during proof tests provided the footbridge modal properties, indicating that the first flexural mode was at a frequency of 1.75 Hz, well within the critical range of excitation due to walking pedestrians. A FE model confirmed this finding. Subsequently, the experimental response of the footbridge to crossing pedestrians was determined for different groups of pedestrians walking at the first mode frequency. The outcome of these tests provides both an experimental assessment of the serviceability conditions and useful insights on the different footbridge response due to the inter- and intra-subject variability.

In the following, Section 1 describes the case study. Section 2 presents the results of operational modal analysis and structural identification, while Section 3 is devoted to the numerical finite element (FE) modelling. Section 4 presents and discusses the forced vibration tests with walking pedestrians. A few conclusions are drawn in Section 5.

1 DESCRIPTION OF THE FOOTBRIDGE

The footbridge, shown in Figure 1, overpasses the Lambro River (Cerro al Lambro, Italy), and runs parallel to a 3-arch masonry Canal Bridge built on 1806. The straight footbridge, 107 m long and 4.4 m wide, is subdivided into a central span, 58 m long, and two side spans, each 24 m long. Two welded double-T longitudinal beams, 2 m high and located at the two sides of the footbridge are its main resisting elements.

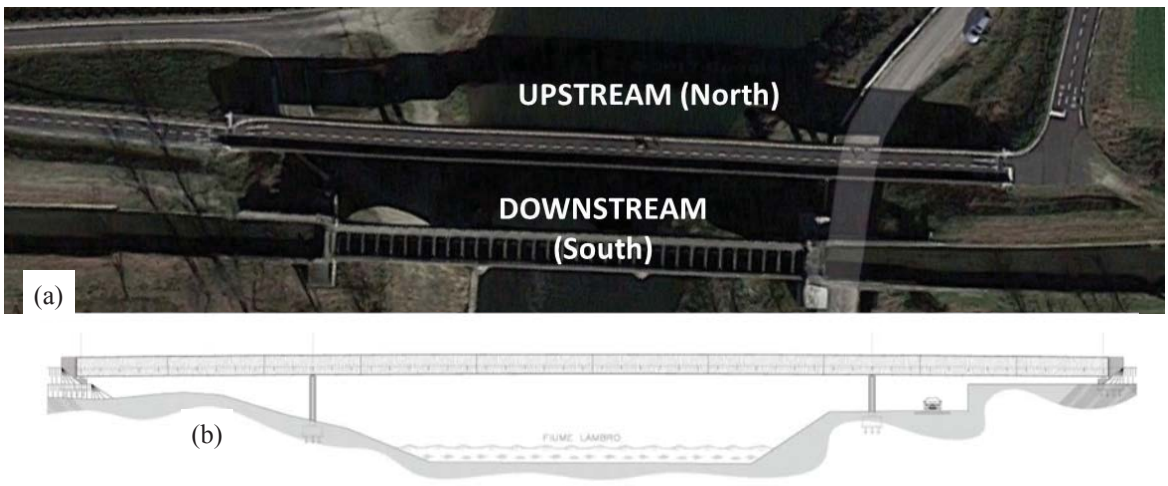

Figure 1: Lambro footbridge: (a) aerial view; (b) side view.

Each longitudinal beam is subdivided in ten on-site welded segments, whose geometry is symmetric about the longitudinal axis and the transverse axis at mid-span. A view from below

of the footbridge and its typical cross-section at an intermediate support are shown in Figure 2a and 2b, respectively. The cross brace system in Figure 2a is made of steel L90×8 profiles bolted at the bottom flange of the longitudinal beams. The same figure also shows the transverse beams and the secondary beam, an IPE100, connecting the mid-span of transverse beams. Figure 2b shows the transverse beam, made of the steel profile IPE240 in the mid-span and of HEA240 on the piles and at the side spans. Transverse beams connect the longitudinal beams and support the deck, where a reinforced concrete (RC) slab with an overlying bituminous conglomerate pavement is cast on a metal corrugated sheet. The deck has an inclination of 2%. As shown in Figure 1b, two couples of circular RC columns provide the intermediate supports subdividing the bridge into three spans. Foundation of columns is on piles. At all supports, the bottom flange of longitudinal beams rest on elastomeric bearings SI-H 300/52. At intermediate supports, a RC 45×45 cm pile cap is interposed between column and beam (Figure 2b).

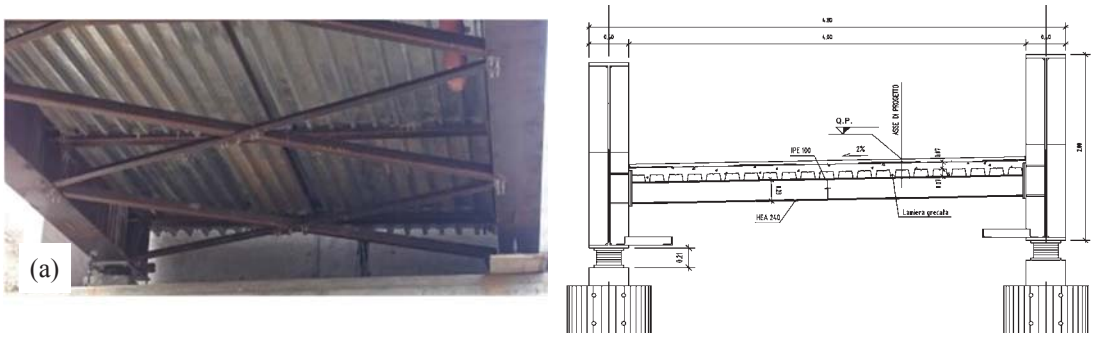

Figure 2: Lambro footbridge: (a) view from below; and (b) cross-section.

With the same corrugated sheet profile A 75/P750 in Figure 3a (units: mm), two cross-sections of the deck are present. In the central span, the sheet thickness is 7/10 mm and the cast in situ slab is 75 mm thick, for a total deck thickness of 150 mm (Figure 3b). At the two ends, for a length of 4.5 m starting from the abutments, the sheet thickness is 15/10 mm and the cast in situ slab is 305 mm thick, for a total thickness of 380 mm. In these zones, where the deck works as a ballast for the central span, the metal sheet is directly connected to the lower flanges of the double-T profiles. Further details on the footbridge geometry can be found in [10].

All steel profiles are made of S335 steel while corrugated sheet is made of S235 steel. Deck is made of concrete of class *C30/37*, having Young's modulus E_c=33 GPa. The class of concrete for columns is *C32/40*, with Young's modulus E_c=33.6 GPa.

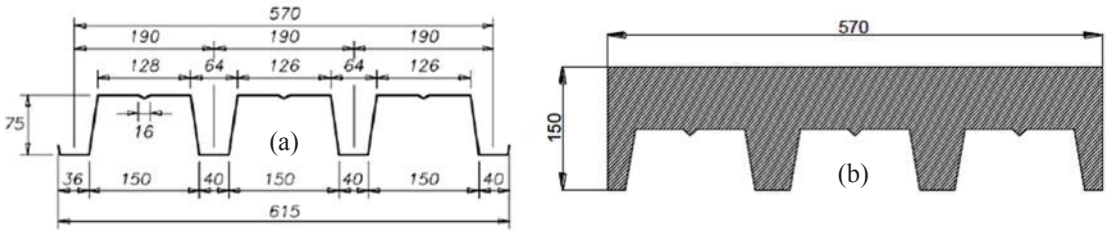

Figure 3: Cross-section of the deck: (a) corrugated sheet A75/P 570; (b) central span, with cast-in-situ concrete.

2 OPERATIONAL MODAL ANALYSIS AND STRUCTURAL IDENTIFICATION

Ambient vibration tests were performed on the footbridge in March 2016 to evaluate its dynamic characteristics. The vertical response was measured in 10 selected points installed on the main side beams (Figure 4), by using high sensitivity piezoelectric accelerometers (WR

model 731A, 10 V/g sensitivity and ±0.50g of peak acceleration). A short cable (1m) connected each sensor to a power unit/amplifier (WR model P31). Two-conductor cables connected the amplifiers to a 24-channel data acquisition system (24-bit resolution, 102 dB dynamic range).

The adopted sampling frequency, in presence of anti-aliasing filters, is equal to 200 Hz, which is fairly larger than that required for the investigated footbridge, as the significant frequency content of collected signals is below 12 Hz (Figure 5). Hence, apart from the already mentioned anti-aliasing filters, the identification tools application was preceded by a second digital step: the time series were low-pass filtered, using a 7th order Butterworth filter with cut-off frequency of 20 Hz, and down-sampled to 40 Hz.

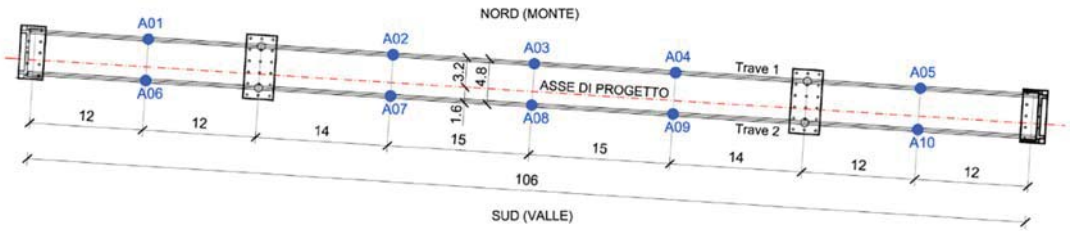

Figure 4: Accelerometer positions on the deck and associated numbers

The modal identification was performed using a time window of 3600 s and applying well-known output-only algorithms, such as the Frequency Domain Decomposition (FDD) [11] and the data-driven Stochastic Subspace Identification (SSI-data) [12] techniques available in the commercial software ARTeMIS [13]. The stabilization diagram, obtained applying the SSI-data algorithm, is shown in Figure 5, along with the first Singular Value (SV) lines of the spectral matrix. The alignments of the stable poles in the stabilization diagram (SSI-data) technique provide a clear indication of the structural modes. Table 1 compares the modal estimates obtained by applying the FDD and the SSI-data techniques through: (a) the identified natural frequencies, f_{FDD} and f_{SSI}; (b) the modal damping ratio and its standard deviation (ζ_{SSI}, σ_ζ) identified by the SSI method and (c) the MAC [14] of the corresponding mode shapes.

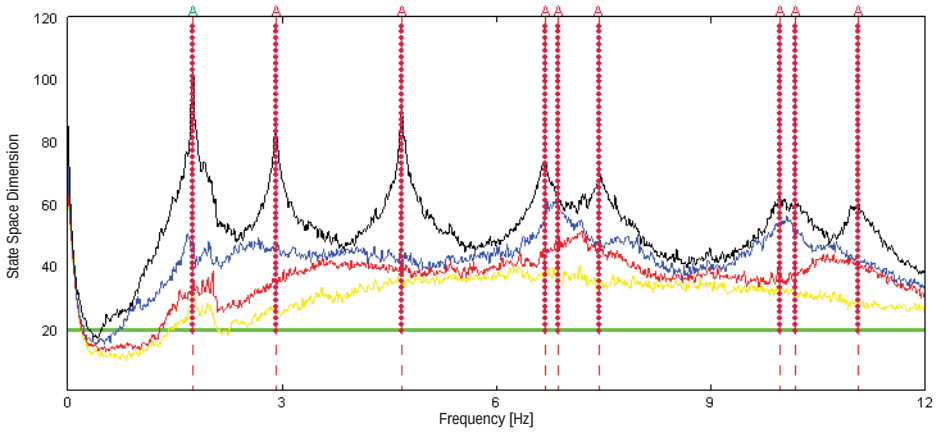

Figure 5: Stabilization diagram (SSI-data) and automatic (A) identification of natural frequencies.

The inspection of Table 1 confirms that the natural frequencies estimated by the two different methods are practically coincident. A similar correspondence was found for most mode shapes (MAC value larger than 0.98), except for the 5th mode (torsion), for which the MAC is about 0.80 and the SSI-data algorithm conceivably provides a better estimation of the mode shape. Figure 6 shows the measurement-based mode shapes identified using the SSI-data technique.

Mode Id.	f_{FDD} (Hz)	f_{SSI} (Hz)	ζ_{SSI} (%)	σ_ζ (%)	MAC
1 (B)	1.748	1.749	0.135	0.83×10^{-3}	1.000
2 (T)	2.910	2.912	0.758	0.81×10^{-2}	1.000
3 (B)	4.668	4.675	0.249	0.13×10^{-2}	1.000
4 (B)	6.660	6.676	1.001	0.35×10^{-2}	0.998
5 (T)	6.797	6.862	3.084	0.34×10^{-2}	0.801
6 (B)	7.441	7.443	1.389	0.79×10^{-2}	0.993
7 (T)	9.954	9.956	1.373	0.16×10^{-1}	0.984
8 (B)	10.190	10.190	1.774	0.71×10^{-2}	0.998
9 (T)	11.030	11.060	1.172	0.21×10^{-1}	0.998

Table 1: Summary of the modal parameters identified by FDD and SSI-data methods (B=bending; T= Torsion).

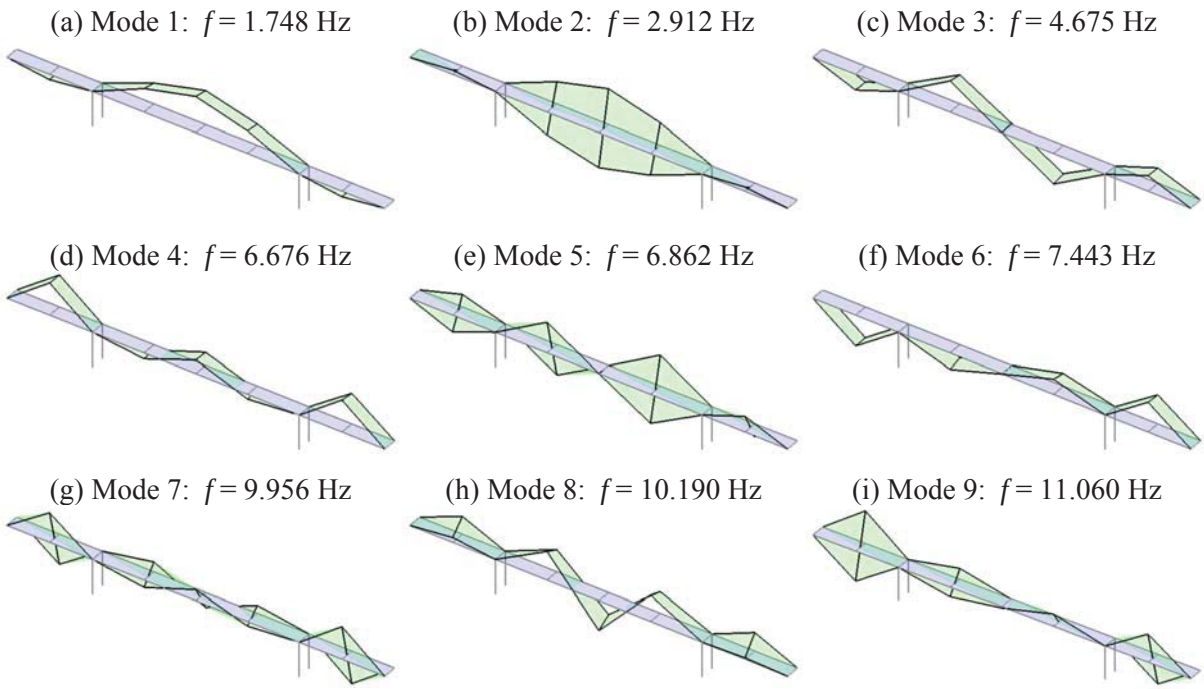

Figure 6: Vibration modes identified from ambient vibration measurements (SSI-data).

3 FINITE ELEMENT MODEL

The finite element (FE) model of the bridge (Figure 7) is based on the as-built design data extracted from the blueprints. The origin of the reference system for the mesh nodes is on the exterior node of the first segment of the upstream side: *x*- and *y*-axis are the transverse and longitudinal axis, respectively, while the *z*-axis is vertical upwards. Within the ANSYS [15] framework, the steel elements are modeled with two-node Timoshenko elements named BEAM188. Shell elements named SHELL181 describe the deck, with a mesh grid of 1m × 1m. Consistent mass option is adopted for all these elements. A BEAM188 element is adopted also for elastomeric bearings, fixed at its lower end and free to rotate differently from the longitudinal beam node it is connected to. Since the deck in the central span is simply supported by

transverse beams, nodes of the shells and nodes of the transverse beams share the same translational degrees of freedom but can have different rotations. The situation is slightly different at the end spans, where the transverse beam are included within the slab thickness and also rotations are constrained.

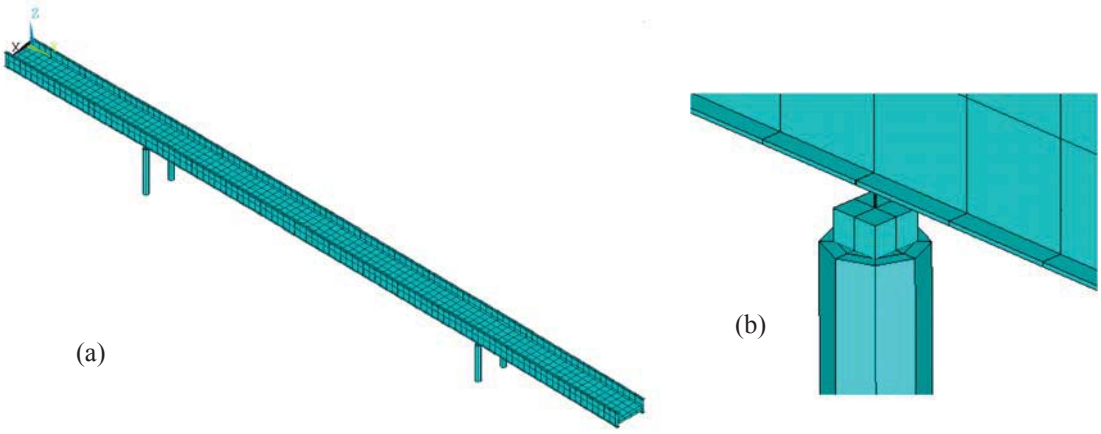

Figure 7: FE model: (a) general view; (b) detail of column with pedestal and elastomeric bearing.

The mesh nodes are located on three different layers, due to the offset among the axes of longitudinal beams, deck, transverse beams and bracing. Thus, in spite of the relatively simple structural scheme, the FE mesh is made complex by the need to account for both offsets and internal releases between adjacent elements. A further problem arises from the orthotropy of the deck, with different values of moments of inertia in longitudinal and transverse direction, due to the shape of the corrugated metal sheet (see Figure 3). SHELL181 elements are characterized by a rectangular cross-section, with a unique value of thickness, density and elastic modulus in both directions. Hence, with a preliminary calibration of these parameters for the two typical cross-sections, an effective shell thickness t_e was determined - equal to 122 mm in the central span and 347 mm for the two side spans - as the one of a rectangular cross-section providing the same moment of inertia of the existing section about the transverse axis. From the t_e value, an effective value of density ρ_e is computed, equal to 3400.7 kg/m^3 in the central span and to 3086.0 kg/m^3 for the two side spans, able to reproduce the total mass of each element, also accounting for dead load. Materials properties have the values defined in Section 1.

3.1 Model updating

A preliminary dynamic analysis on the FE model just presented was performed to check the similarity between experimental and numerical modal parameters. The correlation between the dynamic characteristics of the initial model and the experimental results is shown in column (3) of Table 2 via the frequency discrepancy $\varepsilon_f = (f_{FEM} - f_{SSI})/ f_{SSI}$. Column (4) list the number of order of the numerical mode and a descriptor of the mode shape: bending in the vertical plane (B) or torsional (T). Table 2 shows one-to-one correspondence between the mode shapes and fairly good correlation also in terms of frequency. Only the frequency discrepancy of the second mode is 9.13%, whereas it ranges between –0.76% and 3.35% for the other modes. Hence, the correlation between numerical and experimental behavior seems to provide a sufficient verification of the main assumptions adopted in the initial model.

As previously pointed out, the main uncertainties in the numerical model are related to the footbridge deck and, more specifically, to the Young's modulus of the cast-in-situ concrete (E_{deck}) and to the effective thickness of the shell elements along the span (t_{e1}) and near the

supports (t_{e2}). In order to improve especially the main difference (on the frequency of second mode), the three uncertain parameters of the deck (E_{deck}, t_{e1} and t_{e2}) were updated and their optimal values were identified by minimizing the difference between numerical and experimental natural frequencies. After the updating, a complete correlation analysis was carried out between numerical and experimental modal parameters. The MAC index [14] in column (7) of Table 2 shows an excellent correlation for all the modes. Discrepancy in terms of frequency has a different trend for bending vertical modes, correctly reproduced, and for torsional modes, still affected by an error up to 7.73% for the second mode. Figure 8 shows the numerical counterpart of Figure 6 after updating. The first three numerical modes are "quasi-rigid" modes, transversal, longitudinal and rotational, respectively, involving the bearings deformability. Modes 5 and 9 (f = 1.903 and 6.411 Hz) are lateral/torsional modes and were not identified experimentally.

Exp.	Initial Model			Updated Model		
f_{SSI} (Hz)	f_{FEM} (Hz)	ε_f (%)	Mode #	f_{FEM} (Hz)	ε_f (%)	MAC
1.749	1.749	–	4/B	1.749	–	0.995
2.912	3.178	9.13	6/T	3.137	7.73	0.999
4.675	4.676	0.02	8/B	4.672	–0.06	0.998
6.676	6.702	0.39	10/B	6.683	0.10	0.999
6.862	6.968	1.54	11/T	6.782	–1.17	0.990
7.443	7.508	0.87	12/B	7.483	0.54	0.995
9.956	9.880	–0.76	13/T	9.575	–3.83	0.964
10.190	10.188	–0.02	18/B	10.107	–0.81	0.945
11.060	11.430	3.35	36/T	11.318	2.33	0.974

Table 2: Correlation between experimental and numerical (initial and updated model) dynamic characteristics.

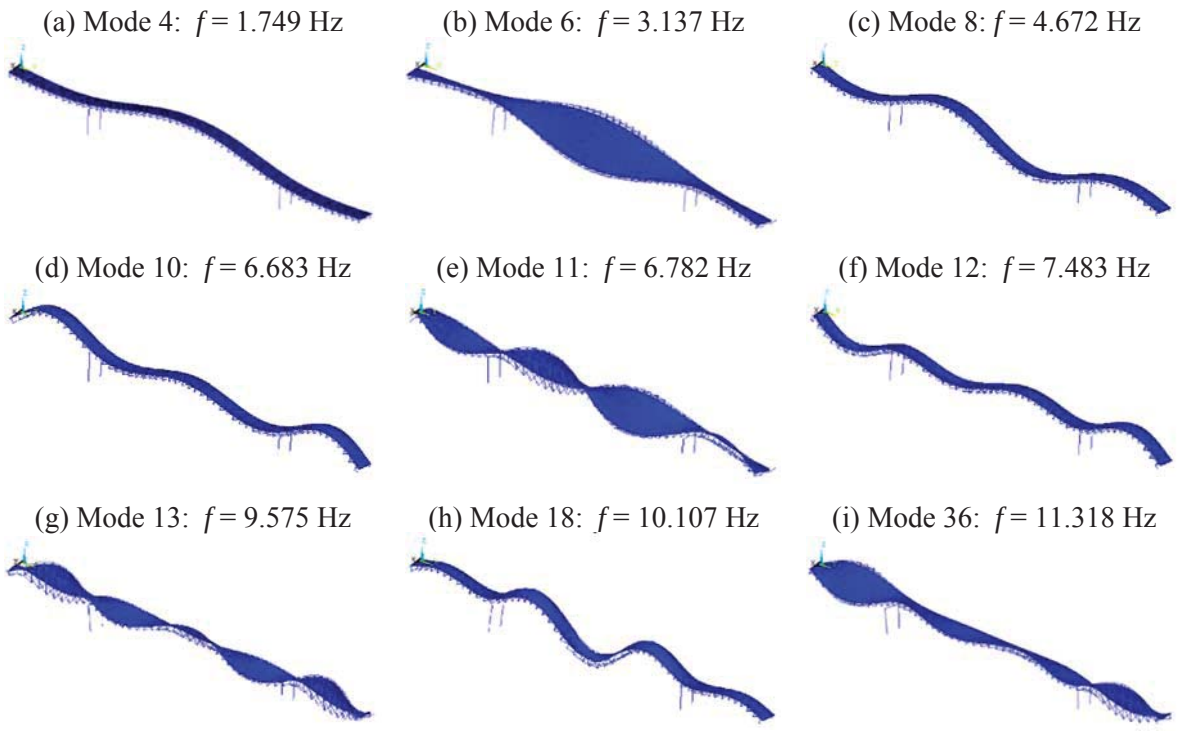

Figure 8: Natural frequencies and mode shapes of the updated FE model.

4 FORCED VIBRATION TESTS

After the proof tests of 2016 and the development of the FE model, a series of forced vibration tests under walking pedestrians were performed on July 20, 2017. Tests aimed to assess the extreme values of the bridge response to different pedestrians' configurations, and the effect of pedestrians' inter-subject variability. Table 3 presents the ID, sex, mass *M* and height *H* of the twelve volunteers involved in the tests (including also two Authors). All TSs are young people, with an age between 22 and 30, but TS5 and TS8, whose age is in the range 50-60. Fifty-two tests with different configurations were performed, involving either single pedestrians or groups with different numbers of people, as detailed in Table 4. Configurations differ either in space or in the Test Subjects (TSs) involved, as it is the case for the twelve configurations with a single pedestrian.

ID	TS1	TS2	TS3	TS4	TS5	TS6	TS7	TS8	TS9	TS10	TS11	TS12
Sex	M	M	F	F	M	F	F	M	M	M	M	M
M [kg]	65	86	59	53	70	65	62	84	76	72	73	70
H [cm]	172	182	164	158	181	173	170	177	185	183	175	175

Table 3: General data of test subjects (TS) involved in the walking tests.

Pedestrians #	1	2	3	4	6	8	12
Configurations	12	6	6	9	4	4	11

Table 4: Number of configurations adopted for each of the different numbers of pedestrians crossing the bridge.

To detect the extreme values of the bridge response, the overall layout of the test was designed to excite mainly the fundamental mode. Hence, for all tests, the target walking frequency of pedestrians was 1.75Hz and spatial configurations were either aligned along or symmetric about the longitudinal axis of the bridge. The first tests involved single pedestrians walking on the bridge, to investigate the uncertainty related to the excitation provided by each individual walking on the bridge. Differences concerns coordination, capability to adapt and follow a predefined rhythm on the 100m distance of the bridge length, as well as the capability to adapt to a lock-in condition when the bridge is vibrating in a perceptible way. In the subsequent tests, the maximum acceleration amplitudes given by groups of walking people arranged in different configurations were investigated. Pedestrians, in groups of 2, 3, 4, 6 or 12 people, were aligned either along the bridge axis, or in a transverse row (with a maximum of 4 people) or in staggered formations with one or more transverse rows and at least two people in each row.

The output produced by the walking people in each configuration was detected in terms of vibration measurements at several points. Figure 9 shows the accelerometer layout. In addition to the sensors used for the modal analysis (see Figure 4), there are four vertical sensors located at the intermediate supports and five horizontal sensors in the central span. The measurement set-up adopted the high sensitivity accelerometers and the data acquisition system of the AVTs.

Individuals or groups of pedestrians crossed the whole bridge, entering from the left side in Figure 9 and exiting on the opposite side. Each crossing corresponded to a single record with multiple channels. Recording of the bridge vibrations started a few instants before the entrance of pedestrians on the bridge and stopped when free vibrations following the transit decayed significantly. To detect the time instant at which each pedestrian started to cross the bridge in the records, each volunteer gave a heel strike while entering the bridge.

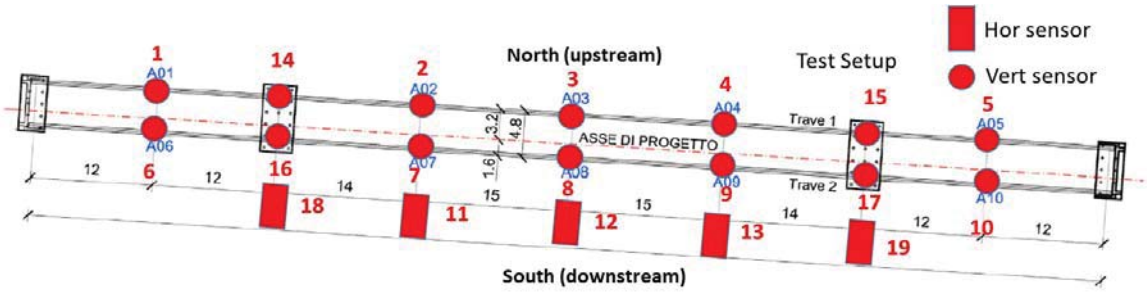

Figure 9: Accelerometer layout during the tests with walking people.

Records of the 19 sensors for the 52 tests show a general trend. The bridge response, in terms of vibration time history, reflects the quasi-symmetry of the bridge. Records on the first half of the bridge almost overlap those on the second half, but the latter show larger acceleration, denoting a resonant phenomenon that builds up during the bridge crossing. Downstream records are similar to but slightly exceed upstream records, possibly due to the effect of the torsional mode. In the following, the presentation of a few results will focus on basic aspects, providing a clear indication of the extreme values of vertical acceleration. A more detailed analysis will concern tests with a single pedestrian, highlighting the effect of intra- and inter-variability.

4.1 Single pedestrian tests

This series of tests aimed at evaluating differences in the excitation produced by each TS. Figure 10 depicts, for each pedestrian, the extreme values recorded by the vertical sensors aligned along the downstream edge during the bridge crossing in the sense from A6 to A10 (see Figure 9). These 12 tests confirm the general trend of the bridge response: the peak values in A6 and A10 are similar but not equal. Values in A10, towards the end of the bridge crossing, exceed those in A6, at the bridge entrance, showing that the resonance phenomenon builds up during the bridge crossing. Sensor A8 at mid-span detects the overall extreme value of the bridge response, reaching 0,30 m/s^2, a value within the comfort range according to Hyvoss Guideline [16]. In addition, the minimum peak value in A8, around 0.06 m/s^2, indicates a wide spread in extreme values produced by different TSs, also visible in the dispersion about the average value (dotted line in Figure 10). The standard deviation (solid lines in Figure 10) has the same pattern of the average value, denoting that dispersion increases as the vibration levels.

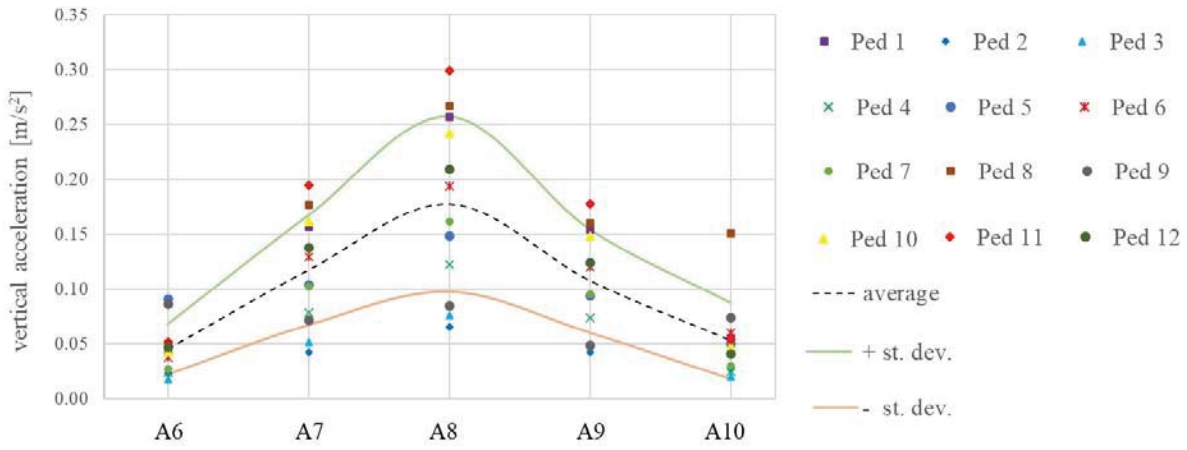

Figure 10: Single pedestrian tests, peak values and standard deviation of vertical downstream acceleration.

Figure 11 shows, for two pedestrians crossing the bridge (TS1 and TS2), the time history of acceleration at the seven downstream vertical sensors, superposed in a single graph. Even though walking at the same frequency, each person has his/her own step speed and, in the three graphs, equal time does not necessarily imply equal position on the bridge. In each graph, the signals of the different sensors differ in amplitude but are eminently in phase. While graph in Figure 11a appears dominated by the first natural mode, more frequency components are visible in Figure 11b where a "beating" phenomenon is appreciated. Largest values are found in the first case. Differences can be justified by the person's capability to keep a constant rhythm (and possibly a centered trajectory) and therefore to excite resonance on the first mode. The excitation under resonant conditions requires some time for the bridge vibrations to reach the maxima, followed by a certain time required for a complete decay, after the person left the bridge.

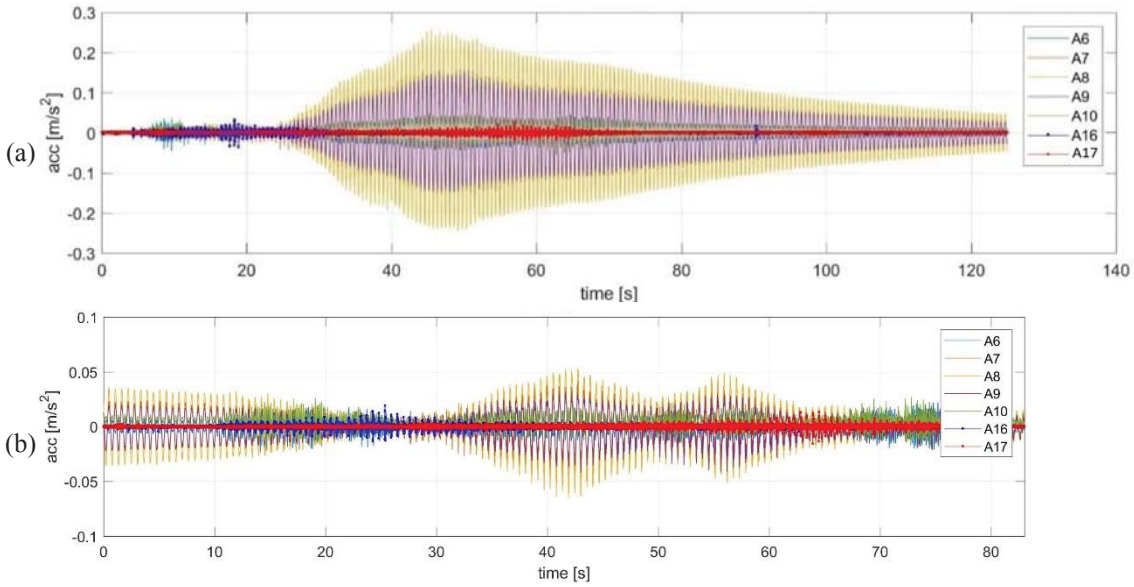

Figure 11: Downstream records for single pedestrians: (a) TS1; (b) TS2.

The trends shown in Figure 10 and Figure 11 can be associated with the different capability of the TSs to lock to the first mode bridge vibration. To investigate this aspect, the time (measured from the beginning of the records) of peak occurrence in downstream sensors is depicted in Figure 12. Two different patterns are apparent: a few pedestrians excite the bridge to high levels while walking on the shorter side spans, while others produce the maximum vibration level in all sensors only when walking close to mid span, where the modal shape allows for the maximum energy input.

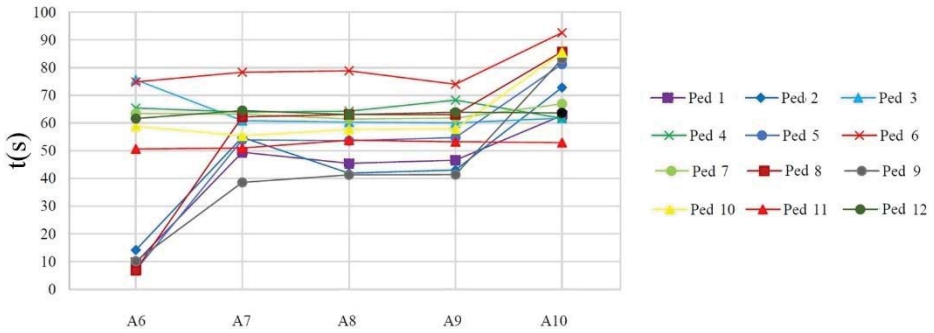

Figure 12: Time at which maxima are reached during each time record (downstream).

Figure 13 and Figure 14 present a time frequency relation for pedestrians TS1 and TS2 at sensors A6 (side span) and A8 (midspan), respectively. Fourier spectra are computed with a moving window, 6 s long, overlapped by 5/6 of the window length. The first natural frequency of the bridge is clearly visible for both people and for both sensors. For both pedestrians the spectral response of the side span includes many higher order harmonics, coherently with the modal shapes at the side span and with the fact that the build up under resonant conditions needs some time to develop fully. The energy dispersion in TS2's response leads to lower values of energy on each frequency and a limited value of vibration (Figure 11b).

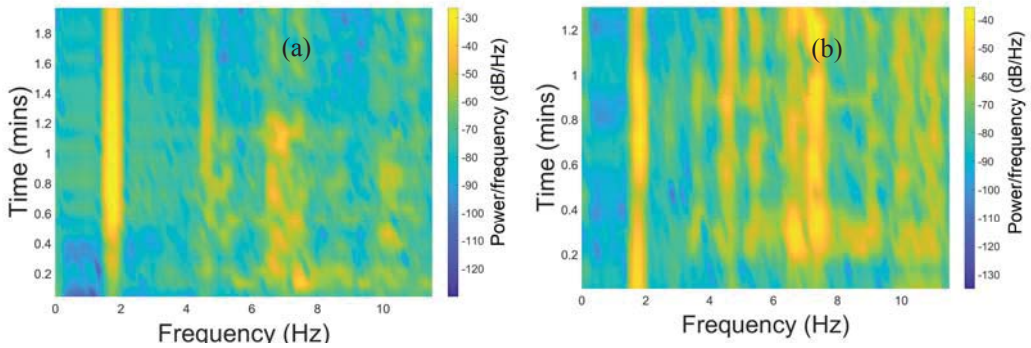

Figure 13: Time frequency representation at sensor A6: (a) TS1; (b) TS2.

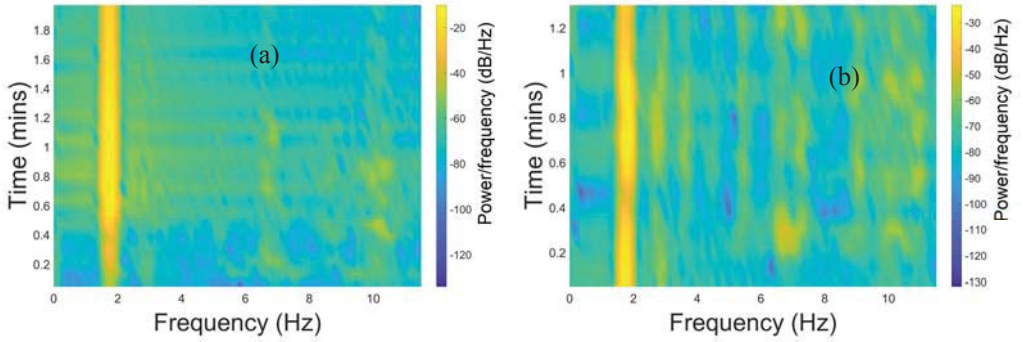

Figure 14: Time frequency representation at sensor A8: (a) TS1; (b) TS2.

A similar pattern is detected at mid-span (Figure 14), where the energy transmitted by TS1 is practically all on the first mode frequency and is associated to significant levels of vibration (see Figure 11a). TS2's response still shows a certain degree of dispersion, even though more limited than that visible in Figure 13b. Again, dispersion is associated to lower values of both energy per frequency and levels of vibration dominated by the first mode.

4.2 Groups

Forty tests concerned groups of two or more pedestrians, as detailed in Table 4. In longitudinal direction, pedestrians were spaced apart of a target distance of 60 cm. In transverse direction, inter distance was not constant, depending on the number of pedestrians involved. For each space configuration of a given group of pedestrians, at least two tests were performed varying the TSs involved. The presentation of these tests is beyond the scope of this paper, and only two aspects are discussed here. First, the average peak value of vertical acceleration at midspan (sensor A8) is investigated in Figure 15, as a function of the number of crossing pedestrians in the same space configuration, a longitudinal row along the bridge axis. The average

is computed for each group of tests concerning the same number of pedestrians. Vertical acceleration increases when the number of pedestrians varies between one and eight, and slightly decreases when pedestrians are 12. The values in Figure 15 can be assumed as a measure of the serviceability conditions of the footbridge.

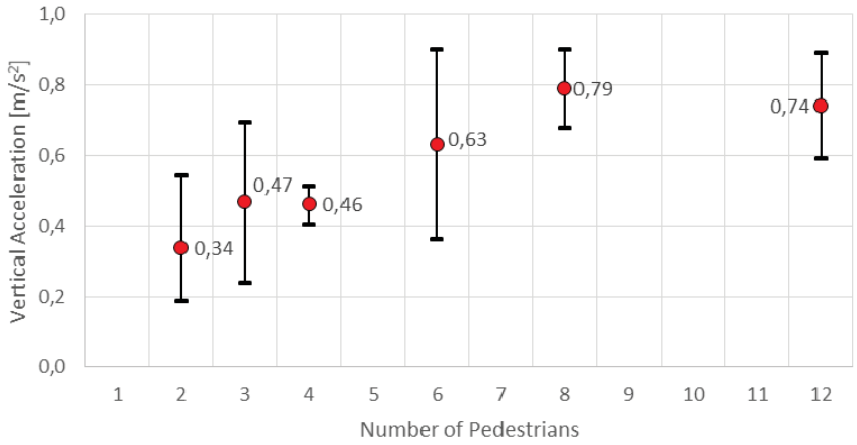

Figure 15 : Average and extreme values of peak acceleration and as a function of the number of pedestrians.

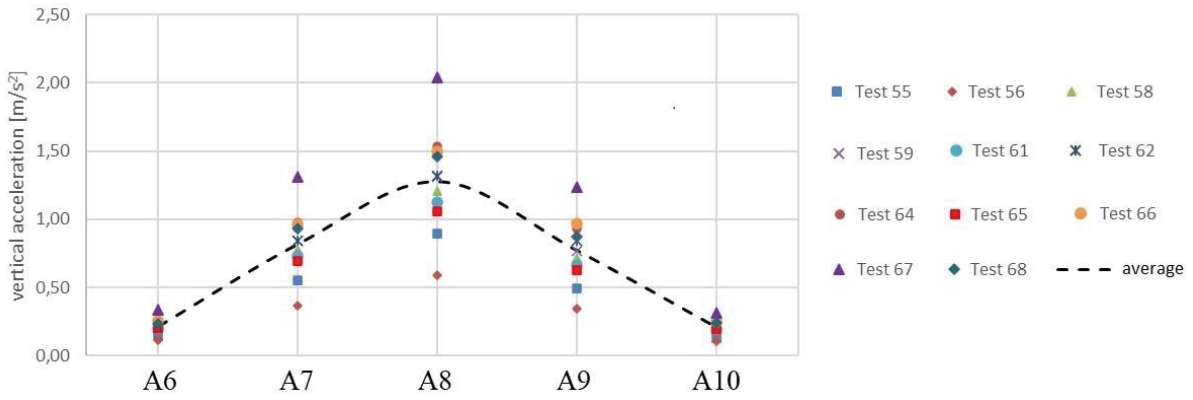

Figure 16: Downstream sensors, peak values for groups of 12 people in different space configurations.

Second, the outcome of the 11 tests with twelve pedestrians in different space configurations is shown in Figure 16 in terms of peak acceleration at downstream sensors. Test 55 and 56 involved a longitudinal row of 12 people. Test 58 and 59 involved two transverse rows of 6 people while Test 61 and 62 had six transverse rows of 2 people. Test 64, 65 and 66 involved four transverse rows of 3 people while Test 67 and 68 had three transverse rows of 4 people.

The most severe load case was generated by Test 67, whose results, however, are quite different from those of Test 68, sharing the same space configuration even though with different positions of pedestrians. While the compact space configuration is able to excite significantly the first mode when all the pedestrians are around midspan where the mode shape has its maximum, the lack (or presence) of synchronization among pedestrians is able to explain both the peak values reached and the difference between Tests 67 and 68.

5 CONCLUSIONS

Aim of this paper was the presentation of selected results on the dynamic testing of a footbridge located in Northern Italy. Experimental tests were performed with different purposes at different times. First, AVT's were carried out in 2016, to identify modal properties, as a part of

proof tests necessary to the footbridge opening. Subsequently, after the derivation of a FE model able to simulate with accuracy the modal properties, forced vibration tests were performed within a sponsored research program. The positive novelty of this work is the link between the two series of tests, where the results of AVTs have driven the subsequent FE modeling and walking tests. The availability of a validated FE model of the footbridge is the base for a future numerical simulation of the walking tests, providing a reliable numerical model of a real structure in the coupled problem of human-structure interaction. Hence, these tests can be adopted to evaluate and validate modelling strategies for pedestrians as mechanical systems moving with a given gait.

The results of numerical modelling showed a problem in reproducing the experimentally detected behavior, relieved but not solved by an optimization procedure. Since vertical bending modes are simulated with an excellent agreement, it appears that the footbridge possesses separated resisting mechanisms in bending and torsion, an aspect that must be tackled in future research works. Foundations on piles, not accounted for in this work, could be the cause of the experimental frequency lower than the numerical one. Their effect is currently under study.

Tests on a limited sample of single pedestrian under similar conditions outlined a meaningful but large spread in their behavior, when trying to walk under resonant conditions. The different response generated by TS1 and TS2, in terms of both peak value and frequency content of vertical acceleration, evidences a dissimilar behavior of the two TSs. Differently from TS2, TS1 locks in to the footbridge vibration, an aspect that should be taken into account when modeling human-structure interaction.

Among the tests performed with groups of pedestrians, in this work only two types of tests are considered. Tests with pedestrians on a single line provides an indirect serviceability assessment, showing an increasing trend with a maximum value as the number of pedestrian increases. Even though in these tests, as in single pedestrian tests, all the peak values are within the range of maximum or medium comfort according to the Hyvoss Guideline [16], it is noticed that a very limited number of pedestrians is able to produce high values of acceleration.

Finally, the results in terms of peak values for the different space configurations of 12 people are analyzed, taking into account that more than one test was performed for each configuration, by varying the position of TSs. At mid-span, the same configuration (the most compact in longitudinal direction) but with different TSs' position produced the overall maximum peak acceleration of the whole test set and the minimum with reference to the configurations of 12 pedestrians. Hence, also in this case two different aspects are brought to the light. First, the importance of the inter-subject variability and of the correlation existing among pedestrians' motion. Second, the need for a numerical serviceability assessment following [16] is confirmed, and is currently under way.

It can be concluded that the experimental research strategy adopted here provided interesting results, opening the way to future numerical and experimental studies.

ACKNOWLEDGEMENTS

The first and last Authors gratefully acknowledge the financial contribution of MIUR (Italian Ministry of Higher Education) under grant PRIN 2015-2018, Project 2015TTJN95, "Identification and monitoring of complex structural systems" for the forced vibration tests of July 2017. The work presented here is based on the MS thesis of G. Lastrico, under the guidance of the other three Authors. AVTs were performed by C. Gentile and forced vibration tests by A. Cigada, with the participation of G. Lastrico and M.G. Mulas. The contribution of V. Racic in devising the pedestrians' configurations is gratefully acknowledged.

REFERENCES

[1] E. Caetano, Á. Cunha, F. Magalhães, C. Moutinho. Studies for controlling human-induced vibration of the Pedro e Inês footbridge, Portugal. Part 1: Assessment of dynamic behaviour, *Engineering Structures*, (32), 1069-1081, 2010.

[2] F. Benedettini, C. Gentile, Operational modal testing and FE model tuning of a cable-stayed bridge, *Engineering Structures*, (33), 2063-2073, 2011.

[3] A. Gheitasi, O. E. Ozbulut, S. Usmani, M. Alipour, D. K. Harris, Experimental and analytical vibration serviceability assessment of an in-service footbridge, *Case Studies in Nondestructive Testing and Evaluation*, (6), 79-88, 2016.

[4] E. Lai, C. Gentile, M.G. Mulas, Experimental and numerical serviceability assessment of a steel suspension footbridge, *J. of Constructional Steel Research*, (132), 16-28, 2017.

[5] I. A. Ribeiro de Silva, J. G. Santos de Silva, Experimental and numerical dynamic structural analysis of footbridges when subjected to pedestrians walking loads, *Journal of Civil Structural Health Monitoring*, 8: 585-595, 2018.

[6] K. Van Nimmen, G. Lombaert, G. De Roeck, P. Van den Broeck, Vibration serviceability of footbridges: evaluation of current codes of practice, *Engineering Structures*, (59), 448-461, 2014.

[7] G. Busca, A. Cappellini, S. Manzoni, M. Tarabini, M. Vanali, Quantification of changes in modal parameters due to the presence of passive people on a slender structure, *J. of Sound and Vibration*, (333), 5641-5652, 2014.

[8] C. C. Caprani, E. Ahmadi, Formulation of human-structure interaction system models for vertical vibration, J. of Sound and Vibration, (377), 346-367, 2016.

[9] M.G. Mulas, E. Lai, G. Lastrico "Coupled Analysis of Footbridge-Pedestrian Dynamic Interaction", *Engineering Structures*, 176C (2018), 127-142.

[10] G. Lastrico, Studio numerico e sperimentale della risposta dinamica di una passerella pedonale, MS Thesis in Civil Engineering, Politecnico di Milano, 2017 (in Italian).

[11] R. Brincker, L.M. Zhang, P. Andersen, Modal identification from ambient responses using Frequency Domain Decomposition, *Proceedings of the 18th IMAC*, 2000.

[12] B. Peeters, G. De Roeck, Reference-based stochastic subspace identification for output-only modal analysis, *Mechanical Systems and Signal Processing* 13(6), 855-878, 1999.

[13] SVS, ARTeMIS Extractor 2011, http://www.svibs.com/, 2012.

[14] R.J. Allemang, D.L. Brown, Correlation coefficient for modal vector analysis, *Proceedings of the 1st IMAC*, 1983.

[15] ANSYS, Online Manuals Release 5.5, http://mostreal.sk/html/guide_55/GBooktoc.html2015.

[16] Research Fund for Coal and Steel. HiVoSS: Design of footbridges, Guideline EN03, 2008.

[17] S. Živanović, A. Pavic, P. Reynolds, Vibration serviceability of footbridges under human-induced excitation: a literature review, *J. Sound Vib*. 279 (1-2) (2005) 1-74.